

## Low expression of microRNA-21 contributes to LPS-induced osteoblast cell apoptosis through up-regulation of *OAS1*

Y. Li<sup>1,✉</sup>, J-L. Jiang<sup>1</sup>, J-S. Yang<sup>1</sup> and L. Gao<sup>2</sup>

<sup>1</sup> Department of Orthopaedics, Nanjing Junxie Hospital, Nanjing, 210002, Jiangsu, China.

<sup>2</sup> College of Life Sciences, Northeast Agricultural University, Harbin 150030, Heilongjiang, China

**Corresponding author:** Ying Li, Department of Orthopaedics, Nanjing Junxie Hospital, Nanjing, 210002, Jiangsu, China. E-mail: [lyingl123ly@126.com](mailto:lyingl123ly@126.com)

### Abstract

Lipopolysaccharide (LPS) is a critical component of the outer membrane of Gram-negative bacteria. Many cellular signals that are activated by Gram-negative bacteria are initiated by LPS. LPS triggers not only inflammatory responses, but also activates pro-apoptotic signals in a series of human cell types. However, there is relatively minimal data on the microRNA-dependent mechanism(s) of LPS-induced functional activity in osteoblast cells. CCK-8 assay and flow cytometry were used to measure cell viability and apoptosis, respectively. RT-PCR and western blot were performed to determine the mRNA and protein expression in osteoblast cells. In this study, we found that LPS triggered apoptosis in osteoblastic hFOB1.19 cells and induced a low expression of the miRNA-21. Furthermore, through the gene microarray technique, *OAS1* was screened and later confirmed to be the target gene which was up-regulated in response to the low expression of miRNA-21. Knockdown of *OAS1* by specific siRNAs significantly rescued the LPS-induced hFOB1.19 cell apoptosis. Our data suggest that LPS induces low expression of miRNA-21 which consequently causes the up-regulation of the downstream gene *OAS1* and eventually triggers apoptosis in hFOB1.19 cells. Knockdown of *OAS1* rescues LPS-induced cell death and thus may be a promising therapeutic strategy for orthopedic diseases.

**Key words:** LPS, miRNA-21, *OAS1*, apoptosis, osteoblast.

### Introduction

Human bone mass homeostasis depends largely on the dynamic balance between the coupled actions of osteoblasts (bone formation) and osteoclasts (bone resorption), termed as bone remodeling (1). Many internal and external pathogens may break the homeostasis and eventually cause pathological diseases, such as osteoporosis and bone cancer. Under these conditions, the programmed cell death (apoptosis) is a well recognized contributor that promotes the progression of diseases (2).

Among the apoptotic factors, lipopolysaccharide (LPS) has been believed to contribute to many cellular signals (3). LPS is derived from the Gram-negative bacteria (e.g. *E. coli*) and originally of interest in various inflammatory responses (4). However, LPS triggers not only inflammatory responses, but also activates pro-apoptotic signals. Toll-like receptor 4 (TLR4) is the main receptor that transduces LPS signals (5,6) and causes the apoptotic cascades in a variety of cell types, including endothelial cells(7,8), epithelial cells (9), macrophages (10) and other immune cells(11,12). However, whether apoptosis could be induced in osteocytes by LPS is not known in literature. And if yes, the mechanisms of how LPS-induced cell death in osteocytes remain to be elucidated.

Recent discoveries of microRNAs (miRNAs) have greatly advanced our knowledge of disease onset. miRNAs are a novel class of regulatory non-coding RNAs that target specific mRNAs for modulation of translation and expression of a targeted protein (13). Of particular interest, multiple miRNAs are aberrantly expressed af-

ter cells exposing to LPS, including miR-155(14), miRNA-15a/16 (13) as well as miRNA-221 (15). In fact, miRNAs have been implicated in several orthopedic disorders (e.g. myelopoiesis and osteosarcoma) (16,17). However, the specific miRNA that was aberrantly expressed in LPS-exposed osteoblastic cells was unclear. One indicative study was that miRNA-21 was reported to be involved in myelopoiesis in primary murine bone marrow stem/progenitor cells (18).

Up-regulation of miRNA-21 has been implicated in carcinogenesis by inhibiting expression of tumor suppressors (19, 20), whereas knockdown of miRNA-21 abolished its oncogenic property (21). Of interest, the functional role of miRNA-21 in these biological processes was accomplished basically through regulation of cell cycle and cell death. Programmed cell death 4 (PDCD4), for example, is directly targeted by miRNA-21 to execute cell death in pancreatic ductal adenocarcinoma (21, 22). There is minimal data, however, that show whether miRNA-21 plays any role in LPS-induced osteoblastic cell activities. And if yes, the downstream targets of miRNA-21 remain to be elucidated.

In the present study, LPS was adopted as a stressor model for induction of cell death in osteoblastic hFOB1.19 cells. We investigated the miRNA-dependent mechanisms of LPS-induced apoptosis, and the rescue pathways used by osteoblast cells to correct cell death. We sought to 1) examine whether exposure to LPS induce hFOB1.19 cell apoptosis, and if yes, 2) assess whether the specific miRNA, i.e. miRNA-21, could be altered in response to LPS treatments, 3) screen the downstream target genes of the specific miRNA using the gene microarray technique and , 4) investigate one

possible pathway that executes the LPS-induced cell apoptosis.

## Materials and methods

### Cells and reagents

The osteoblast hFOB1.19 cells were purchased from the American Type Culture Collection (ATCC, Manassas, VA, USA). Cells were cultured in Dulbecco's Modified Eagle's Medium (DMEM) (Gibco, Grand Island, NY, USA) containing 10% heat-inactivated fetal bovine serum (FBS, Gibco), 10 units/ml penicillin and 10 mg/ml streptomycin (1% penicillin/streptomycin, Thermo Scientific Hyclone) at 37°C in a 5% CO<sub>2</sub> humidified incubator. Culture medium was refreshed every two days. LPS was obtained from Sigma (St. Louis, MO, USA), and dissolved in dimethyl sulfoxide (DMSO) to obtain a 100µg/ml stock solution. The stock solution of LPS was then diluted by DMEM to generate distinct concentrations according to experimental designs. The miR-21 expression plasmid was constructed prior to test by our group. For the western blot analysis, primary antibody against OAS1 was purchased from Abcam (Cambridge, MA, USA). GAPDH was used as the internal loading control with its specific primary antibody from Santa Cruz (Santa Cruz, CA, USA). The corresponding secondary antibody was also purchased from Santa Cruz.

### Transfection

The specific siRNAs against *OAS1* were synthesized by GenePharma Co. (Shanghai, China) and transfected with the lipofectamine 2000 (Invitrogen, Shanghai, China) in accordance with the manufacturer's instructions. The sequences for the specific and control siRNAs were as follows: *OAS1* forward: 5'-GACTGGCG-GCTAAACC-3', reverse: 5'-TTGACTAGGCGGA-TGAGG-3'.

### miRNA isolation

For miRNA-21 expression analysis, total RNAs, including small RNAs, were isolated with the mirVana miRNA Isolation kit (Ambion, Grand Island, NY, USA) according to the manufacturer's instructions. The integrity and quantity of total RNAs (including small RNAs) were assessed with a NanoDrop ND-1000 spectrophotometer (NanoDrop Technologies, Wilmington, DE, USA).

### Western blot

After hFOB1.19 cells exposure to LPS for 24 h, total protein was extracted and quantified with Bio-Rad DC Protein Assay (Bio-Rad, CA, USA). A total of 25µg proteins were loaded to each lane on a 12% SDS-polyacrylamide gel. Subsequently, the protein was transferred to nitrocellulose (NC) membranes for 1.5 h under a voltage of 100v. The membranes were then blocked with 5% skim milk for 1 h and later incubated with primary antibodies at 4 °C overnight. After PBS washes, membranes were then incubated with the secondary HRP-conjugated antibody for 1 h at room temperature. The signals were developed by Super Signal West Pico Chemiluminescent Substrate (Thermo Scientific, MA, USA). The *glyceraldehyde-phosphate dehydrogenase* (*GAPDH*) was synchronously detected for loading

control.

### Quantitative real-time PCR and differential expression gene analyses

Briefly, total RNAs that were isolated (described above) were transcribed into cDNA with SuperScript II (Invitrogen). The cDNA template was then subject to a two-step real time PCR on a Roche LightCycler 480 instrument by using the SYBR green reaction mix (Fisher, Pittsburgh, PA, USA). qRT-PCR reactions were run in triplicate.

For analyses of differential expression genes, the LIMMA package (23) was used in accordance to the manufacturer's instructions. Obtained *p*-values were adjusted for multiple testing using the false discovery rate (FDR) method of Benjamini-Hochberg (B-H). Probe sets were considered as biologically significant if showing a >2 fold change (FC) and a FDR < 0.05. Probe set annotations of gene probe sets were obtained from the Affymetrix NetAffx website (NetAffx release 33.2, <http://www.affymetrix.com/analysis/index.affx>) or the NCBI website (<http://www.ncbi.nlm.nih.gov>). Annotations of miRNA probe sets were derived from the Sanger miRBase database v.20 (June 2013, <http://mirbase.org>).

Unsupervised hierarchical clustering was applied to the microarray expression profiles, using complete linkage and Euclidian distance as a similarity metric, to visualize similarities among probe sets/samples. Both resulting dendrograms were combined in a two-dimensional heat map with color intensities according to the pattern of gene.

### Cell viability measurements

For cell viability measurements, the CCK-8 kit (Donjindo, Japan) was used. In brief, cells with distinct treatments were seeded in a 96-well plate at an initiate density of 4 × 10<sup>3</sup>/well. Cell numbers were monitored in a consecutive of 4 days. For each time point, cells in each well were added with 10µl of CCK-8 solution and incubated for another 2 h at 37°C. Subsequently, absorbance was measured using a synergy 2 multi-mode microplate reader (Bio Tek Instruments, Winooski, VT, USA) at 450 nm. All experiments were carried out in triplicate.

### Apoptosis assays

For apoptosis assessment, the annexin-V/propidium iodide (PI) assay was performed. Briefly, hFOB1.19 cells were plated into 6-well plates (Corning, NY, USA) and incubated with LPS (1 and 10µg/ml) for 48 h. After that, cells from each group were collected, followed by cold PBS washes for twice. The cells were then centrifuged and re-suspended in 100µl of binding buffer that contained 2.5µl FITC-conjugated annexin-V and 1µl PI (100µg/ml), and then incubated for 15 minutes at room temperature under darkness. Data were later analyzed by flow cytometry (BD, San Diego, USA). For the morphological presentation, the fluorometric TUNEL system (Promega DeadEnd™, Madison, WI, USA) was also used to detect apoptotic cells. After staining, cells were visualized under a laser confocal microscopy (Olympus, Japan).

## Statistics

Data were expressed as mean  $\pm$  standard deviation (SD). The Student's *t*-test was used for comparison between groups. The difference was considered significant when a *p*-value  $< 0.05$ .

## Results

### Exposure to LPS inhibits cell proliferation and induces cell apoptosis in hFOB1.19 cells

To determine the effects of LPS exposure on osteoblastic cell growth, we performed the CCK-8 assay for measurements of cell viability in a consecutive of 4 days (Figure 1A). Increasing working concentrations of LPS (1, 10, and 100  $\mu\text{g}/\text{ml}$ ) were employed. It was observed that cells from each group showed proliferative activity during the monitored time point. However, cells treated with LPS had shown prominent growth inhibition as compared with the control group since day 3. On day 4, cells treated with LPS were even more evident from growth inhibition, especially with the LPS concentration of 10  $\mu\text{g}/\text{ml}$ . Cells treated with 1 and 100  $\mu\text{g}/\text{ml}$  of LPS exhibited the similar cell viability on day 4. These results indicated that 10  $\mu\text{g}/\text{ml}$  of LPS had the robust inhibitive effects on hFOB1.19 cell proliferation. To

investigate whether apoptosis underlined the growth inhibition by LPS exposure, the annexin-V/PI assay was performed. Since 10  $\mu\text{g}/\text{ml}$  of LPS had the most effective activity, we only employed 1 and 10  $\mu\text{g}/\text{ml}$  of LPS for treatment of hFOB1.19 cells. The principle is that phosphatidyl serine (PS) translocated from the inner plasma to the outer leaflet of plasma membrane after cells were apoptotic. The exposure of PS to the outer environment in apoptotic cells makes the human anticoagulant, annexin-V strongly bind to PS; therefore leading to the identification of apoptotic cells by the fluorophore or biotin carried by annexin-V. In addition, PI is a red-fluorescent nucleic acid binding dye that exclusively binds tightly to the nucleic acids in dead cells. However, it is impermeable to both live and apoptotic cells. As a result, populations of each kind of cells can be visualized by their fluorescence, and can also easily be distinguished using a flow cytometer. In the scatter plot of double variable flow cytometry, left lower quadrant (FITC<sup>-</sup>/PI<sup>-</sup>) shows living cells; upper right quadrant (FITC<sup>+</sup>/PI<sup>+</sup>) stands for late apoptotic cells; and upper left quadrant (FITC<sup>+</sup>/PI<sup>-</sup>) represents early apoptotic cells. As shown in Figure.1B, a significant dose-dependent increase in the apoptotic cells was observed. This was especially true in the early apoptotic cells. Exposure to 1  $\mu\text{g}/\text{ml}$  of LPS increased early apoptotic cell percentage from 1.47% to 9.99%, whereas 10  $\mu\text{g}/\text{ml}$  of LPS further increased early apoptotic cells by up to 12.5% (Figure. 1B). Morphological changes in the apoptotic cells were also revealed by TUNEL staining. In the control cells unexposed to LPS, the nuclei were round and homogenous red. However, in the LPS-treated groups, significant nuclei fragmentation and chromatin condensation were observed (Figure. 1C). These data suggest that exposure to LPS inhibits hFOB1.19 cell proliferation, but induces cell apoptosis.

### miRNA-21 is lowly expressed in LPS-exposed hFOB1.19 cells

Previously, it was shown that miRNA-21 was critically involved in myelopoiesis in primary murine bone marrow stem/progenitor cells (18). Given that bone marrow stem/progenitor cells share great homology with osteoblasts, we further assessed whether miRNA-21 was associated with LPS-induced osteoblastic cell apoptosis. We found that miRNA-21 was lowly expressed in LPS-treated hFOB1.19 cells. In the cells exposed to 1  $\mu\text{g}/\text{ml}$  of LPS, expression level of miRNA-21 was only 60% of that in control cells. Expression level of miRNA-21 was even approximately 40% of controls when cells were exposed to 10  $\mu\text{g}/\text{ml}$  of LPS (Figure 2). These results suggest that low expression of miRNA-21 may be involved in LPS-treated osteoblasts.

### Low expression of miRNA-21 up-regulates OAS1

miRNAs function as a novel class of small RNAs that target the 3'-untranslated region of mRNA, leading to modulation of specific gene translation. Consequently, we employed the differential expression gene analysis to screen the potential target genes that were up-regulated by low expression of miRNA-21 (Figure 3A and 3B). To this end, we utilized a miR-21 expression plasmid to up-regulate miRNA-21 expression. As shown in Figure 3A and 3B, multiple genes were altered (red repre-

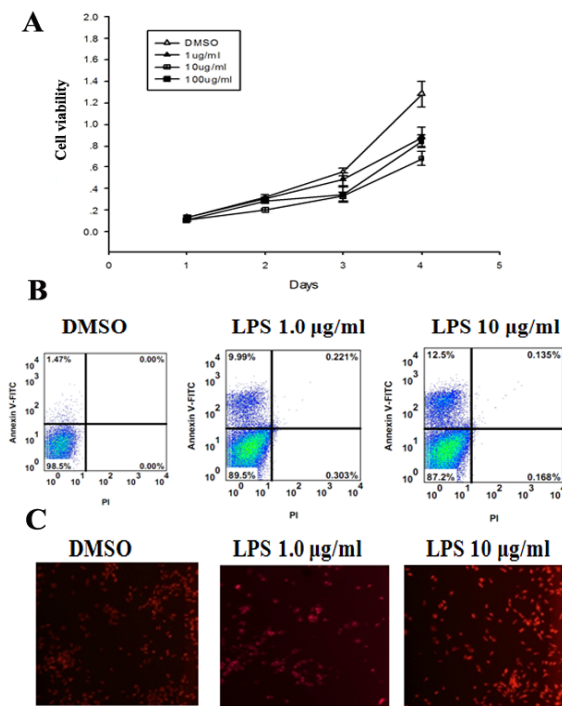


**Figure 1. Exposure to LPS inhibits cell proliferation and induces cell apoptosis in hFOB1.19 cells.** (A) CCK-8 proliferation assay showed that LPS inhibited cell growth as compared with controls. (B) Cell apoptosis was assessed by annexin-V/PI staining, followed by flow cytometry. Left lower quadrant (FITC<sup>-</sup>/PI<sup>-</sup>) shows living cells; upper right quadrant (FITC<sup>+</sup>/PI<sup>+</sup>) stands for late apoptotic cells; and upper left quadrant (FITC<sup>+</sup>/PI<sup>-</sup>) represents early apoptotic cells. Both early and late apoptotic cells were increased compared with control. Exposure to 1  $\mu\text{g}/\text{ml}$  of LPS increased early apoptotic cell percentage from 1.47% to 9.99%, whereas 10  $\mu\text{g}/\text{ml}$  of LPS further increased early apoptotic cells by up to 12.5%. (C) Morphological changes in the apoptotic cells were revealed by TUNEL staining. In the control cells, nuclei were round and homogenous red, whereas LPS-treated cells showed marked chromatin condensation and nuclei fragmentation.

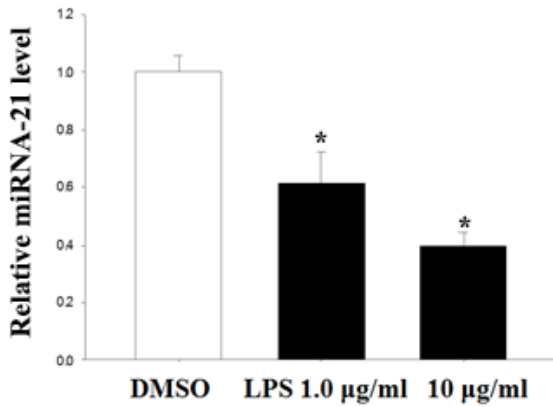


**Figure 2. miRNA-21 is lowly expressed in hFOB1.19 cells exposed to LPS.** In the cells exposed to 1µg/ml of LPS, expression level of miRNA-21 was only 60% of that in control cells. Expression level of miRNA-21 was even approximately 40% of controls when cells were exposed to 10µg/ml of LPS. \* $p < 0.05$ .

sents high expression and blue represents low expression). In the hFOB1.19 cells that were transfected with miR-21 plasmid, some genes were up-regulated (red), while other genes were down-regulated (blue). Furthermore, we performed western blot analysis to confirm the target(s) of miRNA-21, with our focuses mainly on the up-regulated genes (*ACTG2* through *OAS1*). It was observed that down-regulation of *OAS1* expression by miRNA-21 expression plasmid was most prominent among the several potential targets (data not shown). Increasing the concentration of miRNA-21 plasmid significantly decreased the protein level of *OAS1* in a dose-dependent way (Figure 3C). These observations confirm that *OAS1* is one of the targets by miRNA-21.

### Knockdown of *OAS1* rescues LPS-induced cell apoptosis

In view of the results above, we then assessed whether knockdown of *OAS1* interrupted LPS-induced cell death in hFOB1.19 cells. To this end, we synthesized specific siRNAs against *OAS1* (siOAS1). The efficiency of synthesized siOAS1 was first confirmed by qRT-PCR

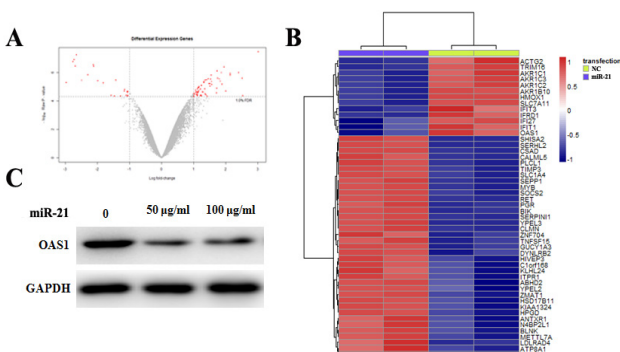


**Figure 3. Low expression of miRNA-21 up-regulates *OAS1*.** (A, B) Differential expression gene analysis was employed to screen the potential targets by miRNA-21. A miR-21 expression plasmid was used to up-regulation expression of miRNA-21. Multiple genes were altered (red represents high expression and blue represents low expression). (C) Western blot analysis confirmed that with the concentration of miRNA-21 plasmid increasing, the protein level of *OAS1* was significantly decreased in a dose-dependent way.

and western blotting which showed that both mRNA and protein levels of *OAS1* was dose-dependently decreased after transfection of siOAS1 (Figure 4A). Based on this, we performed annexin-V/PI to see the effects of *OAS1* knockdown on LPS-induced hFOB1.19 cell apoptosis (Figure 4B, left panel). Knockdown of *OAS1* alone significantly decreased the apoptotic cells compared with control (DMSO+scramble group), which is consistent with previous findings that reported *OAS1* as a pro-apoptotic factor (23). Similar with the data in Figure 1B, Exposure to LPS induced both early apoptosis (10.3% vs. 4.45% in control) and late apoptosis (0.174% vs. 0.135% in control) with the significant changes seen in early stage. More importantly, it was observed that knockdown of *OAS1* significantly attenuated both early and late apoptosis induced by LPS, indicating that knockdown of *OAS1* reversed LPS-induced osteoblasts apoptosis. Moreover, with the CCK-8 kit, cell viability was assessed. And it was observed that knockdown of *OAS1* significantly alleviated LPS-induced cell death. Cell viability in LPS+siOAS1 group was significantly higher than the counterparts (Figure 4C). These data suggest that *OAS1* was critically involved in LPS-induced cell apoptosis.

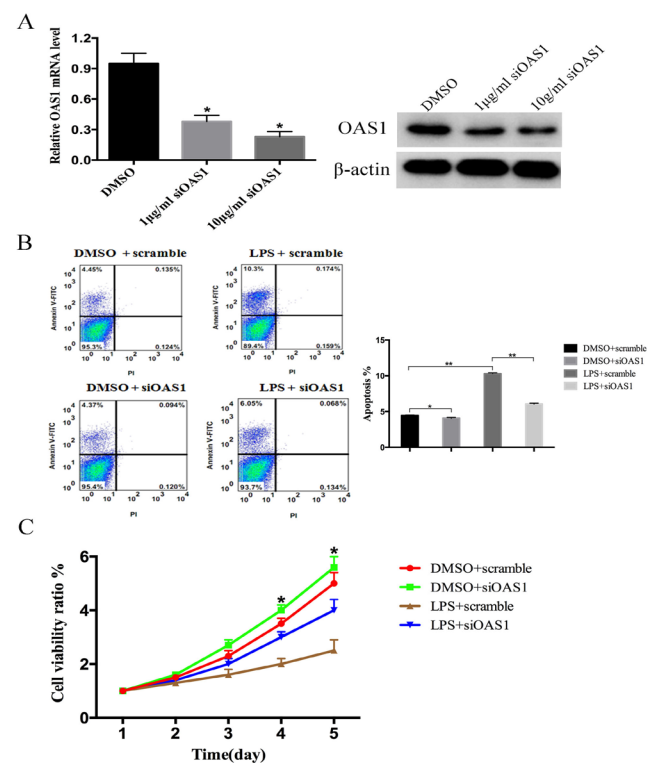


**Figure 4. Knockdown of *OAS1* rescues LPS-induced cell apoptosis.** (A) A specific siRNA against *OAS1* (siOAS1) was synthesized. The knockdown efficiency was confirmed by qRT-PCR (left panel) and western blotting (right panel) which showed that the expression of *OAS1* was dose-dependently decreased after transfection of siOAS1. \*  $p < 0.05$ . (B) The effects of *OAS1* knockdown on LPS-induced cell apoptosis. Knockdown of *OAS1* alone decreased cell apoptosis, and more importantly, reversed LPS-induced hFOB1.19 cell early and late apoptosis. (C) Effects of *OAS1* knockdown on LPS-mediated hFOB1.19 cell growth inhibition. LPS-treated cells showed slower growth rate, while LPS-treated cells with siOAS1 transfection showed more active proliferative rate as compared with scramble siRNA transfection.

## Discussion

Lipopolysaccharide (LPS) has been widely implicated in the pathogenesis of multiple cell deaths associated with Gram-negative bacterial infections (7-11). LPS initiates the formation of a death-related signaling at the cell surface by transducing signals to its receptor TLR-4 on the surface of cells (5,6). The subsequent signaling pathways that execute cell apoptosis remain unclear and may differ among cell types from different systems. In the present study, we investigated the role of LPS in osteoblastic cell survival and more importantly, the subsequent signalings that transduce LPS-mediated osteoblastic cell activity, with the major focus on the miRNA-21 pathways.

In the cell proliferation assay, we found that osteoblasts were dose-dependently inhibited from cell growth by LPS. The growth arrest was due to the increased cell percentages of both early and late stage of apoptosis. These results suggest that LPS could also induce cell apoptosis in osteoblastic cells as it does elsewhere. Furthermore, miRNA-21 is reported to be critically involved in myelopoiesis in primary murine bone marrow stem/progenitor cells (18), indicating the pivotal role of miRNA-21 in bone growth. Herein we provided evidence that miRNA-21 was aberrantly expressed in LPS-induced osteoblastic cell apoptosis. Through a gene microarray technique, we screened and later confirmed that *OAS1* was the target gene that responded to the aberrant expression of miRNA-21 induced by LPS.

*OAS1* belongs to a protein family that consists of enzymes capable to catalyze the synthesis of 2'-5'-linked oligomers of adenosine from ATP (2-5A) (24). The products of these enzymes (2-5A) could bind to the latent Ribonuclease L (RNase L), making the latter subsequently dimerize into the active form. Upon activation, the RNase L functions to cleave both cellular and viral mRNAs, and therefore causes the ribotoxic stress and Janus tyrosine kinase (JNK) activation. All these processes eventually resulted in the inhibition of viral replication, degradation of virus RNA, or promotion of apoptosis cascades (25,26). In fact, *OAS1*-mediated apoptosis have been observed in both human prostate and breast cancer cell lines (26-29). *OAS1*-mediated apoptosis might also be involved in the cell injury by radiation treatments (30). In addition, the mitochondria-involved process exacerbated the *OAS1*-mediated apoptosis (23). Based on these findings, we believe that up-regulation of *OAS1* by the low expression of miRNA-21 was causable to the subsequent apoptosis induced by LPS. This could also be explained by our functional experiments that knockdown of *OAS1* rescued the LPS-induced cellular apoptosis in hFOB1.19 cells.

The LPS-induced *OAS1* signaling was only minimally indicated in the past. One existing study showed that LPS treatment activated IFN-stimulated gene factor 3 (ISGF3) and induced expression of IFN-stimulated genes (ISGs) such as *OAS1*, *DDX58 (RIG-I)*, *MX1*, and *IFIH1 (MDA5)* in human wild-type macrophages (31). Another indicative study reported that LPS could functionally induced expression of (2'-5') oligoadenylate synthetase (*OAS*) in the marine sponges (32). No data were provided on the mechanisms of how LPS induced *OAS1* expression. Our findings, nevertheless,

provided a novel insight into this process, with the focus on miRNA-21. With the low expression of miRNA-21, exposure to LPS caused significant up-regulation of *OAS1* which possibly transduced the apoptotic signals. The identification of miRNA-21 as the key mediator of LPS-induced *OAS1* expression and the eventual apoptosis in hFOB1.19 cells would advance our understanding of osteoblastic cell apoptosis under physiological and pathological conditions.

In conclusion, we studied the role of LPS in osteoblasts and one of the contributory mechanisms. The miRNA-21/*OAS1* signaling is a novel pathway identified here which contributes to LPS-induced cellular apoptosis in hFOB1.19 cells. Knockdown of *OAS1* significantly rescued LPS-induced apoptosis and therefore, might be a promising therapeutic strategy for orthopedic diseases.

## References

- Boyle, W.J., Simonet, W.S., Lacey, D.L. Osteoclast differentiation and activation. *Nature*. 2003; **423**:337-342.
- Chang, E.J., Kim, H.H., Huh, J.E., Kim, I.A., Seung, K.J., Chung, C.P., Kim, H.M. Low proliferation and high apoptosis of osteoblastic cells on hydrophobic surface are associated with defective Ras signaling. *Exp Cell Res*. 2005; **303**:197-206.
- Song, X., Guo, M., Wang, T., Wang, W., Cao, Y., Zhang, N. Geniposide inhibited lipopolysaccharide-induced apoptosis by modulating TLR4 and apoptosis-related factors in mouse mammary glands. *Life Sci*. 2014; **119**:9-17.
- Lowe, A.P., Thomas, R.S., Nials, A.T., Kidd, E.J., Broadley, K.J., Ford, W.R. Lipopolysaccharide exacerbates functional and inflammatory responses to ovalbumin and decreases sensitivity to inhaled fluticasone propionate in a guinea-pig model of asthma. *Br J Pharmacol*. 2015; **172**(10):2588-2603.
- Hoshino, K., Takeuchi, O., Kawai, T., Sanjo, H., Ogawa, T., Takeda, Y., Takeda, K., Akira, S. Cutting edge: Toll-like receptor 4 (TLR4)-deficient mice are hyporesponsive to lipopolysaccharide: Evidence for TLR4 as the *Lps* gene product. *J Immunol*. 1999; **162**:3749-3752.
- Kaiser, W.J., Offermann, M.K. Apoptosis induced by the toll-like receptor adaptor TRIF is dependent on its receptor interacting protein homotypic interaction motif. *J Immunol*. 2005; **174**:4942-4952.
- Hull, C., McLean, G., Wong, F., Duriez, P.J., Karsan, A. Lipopolysaccharide signals an endothelial apoptosis pathway through TNF receptor-associated factor 6-mediated activation of c-Jun NH2-terminal kinase. *J Immunol*. 2002; **169**:2611-2618.
- Wang, H.L., Akinci, I.O., Baker, C.M., Ulrich, D., Bellmeyer, A., Jain, M., Chandel, N.S., Mutlu, G.M., Budinger, G.R. The intrinsic apoptotic pathway is required for lipopolysaccharide-induced lung endothelial cell death. *J Immunol*. 2007; **179**:1834-1841.
- Yu, L.C., Flynn, A.N., Turner, J.R., Buret, A.G. SGLT-1-mediated glucose uptake protects intestinal epithelial cells against LPS-induced apoptosis and barrier defects: A novel cellular rescue mechanism? *Faseb J*. 2005; **19**:1822-1835.
- Xaus, J., Comalada, M., Villedor, A.F., Lloberas, J., Lopez-Soriano, F., Argiles, J.M., Bogdan, C., Celada, A. LPS induces apoptosis in macrophages mostly through the autocrine production of TNF-alpha. *Blood*. 2000; **95**:3823-3831.
- Ardeshtna, K.M., Pizzey, A.R., Devereux, S., Khwaja, A. The PI3 kinase, p38 SAP kinase, and NF-kappaB signal transduction pathways are involved in the survival and maturation of lipopolysaccharide-stimulated human monocyte-derived dendritic cells. *Blood*.

2000;**96**:1039-1046.

12. Kato, Y., Morikawa, A., Sugiyama, T., Koide, N., Jiang, G.Z., Takahashi, K., Yokochi, T. Role of tumor necrosis factor-alpha and glucocorticoid on lipopolysaccharide (LPS)-induced apoptosis of thymocytes. *FEMS Immunol Med Microbiol.* 1995;**12**:195-204.

13. Moon, H.G., Yang, J., Zheng, Y., Jin Y. MiR-15a/16 regulates macrophage phagocytosis after bacterial infection. *J Immunol.* 2014; **193**:4558-4567.

14. Ruggiero, T., Trabucchi, M., De Santa, F., Zupo, S., Harfe, B.D., McManus, M.T., Rosenfeld, M.G., Briata, P., Gherzi, R. LPS induces KH-type splicing regulatory protein-dependent processing of microRNA-155 precursors in macrophages. *Faseb J.* 2009; **23**:2898-2908.

15. Lai, N.S., Yu, H.C., Chen, H.C., Yu, C.L., Huang, H.B., Lu, M.C. Aberrant expression of microRNAs in T cells from patients with ankylosing spondylitis contributes to the immunopathogenesis. *Clin Exp Immunol.* 2013; **173**:47-57.

16. Calin, G.A., Croce, C.M. MicroRNA signatures in human cancers. *Nat Rev Cancer.* 2006; **6**:857-866.

17. Kafchinski, L.A., Jones, K.B. MicroRNAs in osteosarcomagenesis. *Adv Exp Med Biol.* 2014; **804**:119-127.

18. Velu, C.S., Grimes, H.L. Utilizing antagomiR (antisense microRNA) to knock down microRNA in murine bone marrow cells. *Methods Mol Biol.* 2012; **928**:185-195.

19. Si, M.L., Zhu, S., Wu, H., Lu, Z., Wu, F., Mo, Y.Y. MiR-21-mediated tumor growth. *Oncogene.* 2007; **26**:2799-2803.

20. Liu, M., Tang, Q., Qiu, M., Lang, N., Li, M., Zheng, Y., Bi, F. MiR-21 targets the tumor suppressor RhoB and regulates proliferation, invasion and apoptosis in colorectal cancer cells. *Febs Lett.* 2011; **585**:2998-3005.

21. Bhatti, I., Lee, A., James, V., Hall, R.I., Lund, J.N., Tufarelli, C., Lobo, D.N., Larvin, M. Knockdown of microRNA-21 inhibits proliferation and increases cell death by targeting programmed cell death 4 (PDCD4) in pancreatic ductal adenocarcinoma. *J Gastrointest Surg.* 2011; **15**:199-208.

22. Frankel, L.B., Christoffersen, N.R., Jacobsen, A., Lindow, M., Krogh, A., Lund, A.H. Programmed cell death 4 (PDCD4) is an important functional target of the microRNA miR-21 in breast cancer cells. *J Biol Chem.* 2008; **283**:1026-1033.

23. Smyth, G.K. Linear models and empirical bayes methods for assessing differential expression in microarray experiments. *Stat Appl*

*Genet Mol Biol.* 2004; **3**:e3.

24. Domingo-Gil, E., Esteban, M. Role of mitochondria in apoptosis induced by the 2-5A system and mechanisms involved. *Apoptosis.* 2006; **11**:725-738.doi: 10.1007/s10495-006-5541-0.

25. Coffey, E.T. Nuclear and cytosolic JNK signalling in neurons. *Nat Rev Neurosci.* 2014; **15**:285-299. doi:10.1038/nrn3729.

26. Mullan, P.B., Hosey, A.M., Buckley, N.E., Quinn, J.E., Kennedy, R.D., Johnston, P.G., Harkin, D.P. The 2, 5 oligoadenylate synthetase/RNaseL pathway is a novel effector of BRCA1- and interferon-gamma-mediated apoptosis. *Oncogene.* 2005; **24**:5492-5501.doi: 10.1038/sj.onc.1208698.

27. Xiang, Y., Wang, Z., Murakami, J., Plummer, S., Klein, E.A., Carpten, J.D., Trent, J.M., Isaacs, W.B., Casey, G., Silverman, R.H. Effects of RNase L mutations associated with prostate cancer on apoptosis induced by 2', 5'-oligoadenylates. *Cancer Res.* 2003; **63**:6795-6801.

28. Malathi, K., Paranjape, J.M., Ganapathi, R., Silverman, R.H. HPC1/RNASEL mediates apoptosis of prostate cancer cells treated with 2', 5'-oligoadenylates, topoisomerase I inhibitors, and tumor necrosis factor-related apoptosis-inducing ligand. *Cancer Res.* 2004; **64**:9144-9151.doi: 10.1158/0008-5472.CAN-04-2226.

29. Maia, C.J., Socorro, S., Schmitt, F., Santos, C.R. Characterization of oligoadenylate synthetase-1 expression in rat mammary gland and prostate: Effects of 17beta-estradiol on the regulation of OAS1g in both tissues. *Mol Cell Biochem.* 2008; **314**:113-121.doi: 10.1007/s11010-008-9771-z.

30. Tsai, M.H., Cook, J.A., Chandramouli, G.V., DeGraff, W., Yan, H., Zhao, S., Coleman, C.N., Mitchell, J.B., Chuang, E.Y. Gene expression profiling of breast, prostate, and glioma cells following single versus fractionated doses of radiation. *Cancer Res.* 2007; **67**:3845-3852.doi: 10.1158/0008-5472.CAN-06-4250.

31. Sheikh, F., Dickensheets, H., Gamero, A.M., Vogel, S.N., Donnelly, R.P. An essential role for IFN-beta in the induction of IFN-stimulated gene expression by LPS in macrophages. *J Leukoc Biol.* 2014; **96**:591-600.doi: 10.1189/jlb.2A0414-191R.

32. Grebenjuk, V.A., Kuusksalu, A., Kelve, M., Schutze, J., Schroder, H.C., Muller, W.E. Induction of (2'-5') oligoadenylate synthetase in the marine sponges *Suberites domuncula* and *Geodia cydonium* by the bacterial endotoxin lipopolysaccharide. *Eur J Biochem.* 2002; **269**:1382-1392.